Biochemical characterization and NMR studies of the nucleotide-binding domain 1 of multidrug-resistance-associated protein 1: evidence for interaction between ATP and Trp^{653}

Odile RAMAEN*, Sandrine MASSCHELEYN*, Francis DUFFIEUX*[1], Olivier PAMLARD*, Marine OBERKAMPF†[2], Jean-Yves LALLEMAND*, Véronique STOVEN‡[3,4] and Eric JACQUET*[4]

*Institut de Chimie des Substances Naturelles, Centre National de la Recherche Scientifique (CNRS) Unité Propre de Recherche 2301, Avenue de la Terrasse, 91198 Gif-sur-Yvette Cedex, France, †Groupe de Résonance Magnétique Nucléaire, Institut de Chimie des Substances Naturelles, Ecole Polytechnique, 91128 Palaiseau Cedex, France, and ‡Laboratoire de RMN des Biomolécules, Institut Pasteur, 28 rue du Docteur Roux, 75724 Paris Cedex, France

Multidrug-resistance-associated protein 1 (MRP1/ABCC1) is a human ATP-binding cassette transporter that confers cell resistance to antitumour drugs. Its NBDs (nucleotide-binding domains) bind/hydrolyse ATP, a key step in the activation of MRP1 function. To relate its intrinsic functional features to the mechanism of action of the full-size transporter, we expressed the N-terminal NBD1 domain (Asn^{642} to Ser^{871}) in *Escherichia coli*. NBD1 was highly purified under native conditions and was characterized as a soluble monomer. ^{15}N-labelling allowed recording of the first two-dimensional NMR spectra of this domain. The NMR study showed that NBD1 was folded, and that Trp^{653} was a key residue in the NBD1–ATP interaction. Thus, interaction of NBD1 with ATP/ADP was studied by intrinsic tryptophan fluorescence. The affinity for ATP and ADP were in the same range ($K_{d(ATP)} = 118$ μM and $K_{d(ADP)} = 139$ μM). Binding of nucleotides did not influence the monomeric state of NBD1. The ATPase activity of NBD1 was magnesium-dependent and very low [V_{max} and K_m values of 5×10^{-5} pmol of ATP $\cdot$ (pmol NBD1)$^{-1} \cdot$ s^{-1} and 833 μM ATP respectively]. The present study suggests that NBD1 has a low contribution to the ATPase activity of full-length MRP1 and/or that this activity requires NBD1–NBD2 heterodimer formation.

Key words: ABC (ATP-binding cassette), ATP binding and hydrolysis, biochemical and NMR studies, MRP1/ABCC1 (multidrug-resistance-associated protein 1), nucleotide-binding domain.

INTRODUCTION

Multidrug-resistance-associated protein 1 (MRP1/ABCC1) belongs to the ABC (ATP-binding cassette) protein family [1], and its overexpression confers multidrug resistance [2]. This phenotype, similar to that observed in cells overexpressing P-glycoprotein (MDR1/ABCB1), another member of the ABC family [1,3], is one of the major causes of failure in cancer chemotherapy (see [4] for a review).

MRP1 presents the same global topology of most ABC transporters, consisting of a repeat of transmembrane domains, and NBDs (nucleotide-binding domains) characterized by the presence of Walker A, Walker B and ABC signature consensus sequences. However, MRP1 also contains an additional N-proximal transmembrane domain and an extracytosolic N-terminus [5]. It is believed that MRP1 functions as an energy-dependent efflux pump controlled by the hydrolysis of ATP, but we lack information on the mechanism that couples ATP binding and hydrolysis at the NBDs and drug transport. The aim of the present study was to elucidate the intrinsic properties of the NBD1 domain of MRP1 and to relate it to the function of the full-length transporter. The NBDs seem to play a central role in the activation–dimerization process of MRP1 [6,7].

Similar approaches have been developed on isolated NBDs from ABC transporters, but only few studies have focused on the NBDs from MRP1 expressed as recombinant proteins in insect cells [6] or in *Escherichia coli* [8–10]. Most of those studies were limited by their inability to express or purify large amounts of recombinant domains, by the need to use fusion proteins to produce soluble chimaera and by their tendency to form large aggregates. These limitations have been overcome in the present study for the NBD1 domain of MRP1, providing efficiently a high amount of purified soluble protein. This allowed the biochemical characterization of NBD1 and study of its interaction with nucleotides by NMR and fluorescence. Discussion of our results pertains specifically to the biochemical properties of isolated NBDs and their role in full-length transporters.

MATERIALS AND METHODS

Construction of the recombinant NBD1 expression vector

Total RNAs were purified from the human cell line HL60/ADR (Oncodesign, Dijon, France), using the High Pure RNA Isolation Kit (Roche Molecular Biochemicals, Meylan, France). Reverse transcriptase–PCR amplification of the NBD1 cDNA fragment was performed with the Titan one-tube reverse transcriptase–PCR system (Roche). The forward primer 5′-aattaatagcatcaccgtgag-3′ and the reverse primer 5′-gcggccgctcagctggcatagg-3′ were used, where underlined bases correspond to the *Ase*I and *Not*I restriction sites respectively. PCR fragments were cloned into T-overhanging pBlueScript and subcloned into pET28a (Novagen, Madison,

Abbreviations used: ABC, ATP-binding cassette; CFTR, cystic fibrosis transmembrane conductance regulator; HisP, histidine permease; MBP, maltose-binding protein; 2ME, 2-mercaptoethanol; MRP1, multidrug-resistance-associated protein 1; NBD1, N-terminal nucleotide-binding domain; IPTG, isopropyl-1-thio-β-D-galactopyranoside; TROSY, transverse relaxation-optimized spectroscopy.

[1] Present address: Aventis Pharma, Protein Production and Engineering, 102 route de Noisy, 93235 Romainville Cedex, France.
[2] Present address: Institut Curie, 25 rue d'Ulm, 75005 Paris, France.
[3] To whom correspondence should be addressed (e-mail vstoven@pasteur.fr).
[4] These authors contributed equally to this work.

WI, U.S.A.), using appropriate enzymes (the *Ase*I end of NBD1 cDNA being compatible with the *Nde*I end of pET28a). The final expression plasmid construct was sequenced. The pET28a vector allows the expression of an N-terminal His-tagged fused NBD1 protein (Asn^{642} to Ser^{871}).

Overexpression and protein production

The *E. coli* BL21(DE3)pLysS (Novagen) was transformed with recombinant pET28a-NBD1-MRP1 vector and grown at 37 °C in yeast extract tryptone (2YT) medium (Difco, West Molesey, Surrey, U.K.) containing kanamycin (30 μg/ml) and chloramphenicol (34 μg/ml) until the absorbance at 600 nm reached a value of 0.6 unit. Gene expression was induced with 0.5 mM IPTG (isopropyl-1-thio-β-D-galactopyranoside; Promega, Charbonnières, France) for 20 h at 16 °C (A_{600} 6–7). Then, cells were harvested by centrifugation (10 000 ***g*** for 15 min) at 4 °C, frozen in liquid nitrogen and stored at − 80 °C until use. For the production of the ^{15}N-labelled domain for NMR studies, expression was performed in minimal M9 medium containing 0.1 % [^{15}N]ammonium chloride (Cambridge Isotope Laboratories, Andover, MA, U.S.A.) as the sole source of nitrogen. The production of recombinant domain was induced at a cell density of 0.4 unit at 600 nm and continued overnight at 28 °C.

Protein purification

All purification steps were performed at 4 °C. The cell pellet from 2 litres of culture was resuspended in 60 ml of buffer A (25 mM Tris/HCl, pH 8.0/500 mM NaCl/2 mM $MgCl_2$/1 mM Pefabloc-SC). Cells were lysed by sonication (5 s on/5 s off, 36 cycles) in a Vibro cell sonicator (Fisher Bioblock Scientific, Illkirch Cedex, France) and ultracentrifuged at 200 000 ***g*** for 60 min to sediment the non-soluble fraction of the cell extract. The supernatant was filtered (0.45 μM Minisart; Sartorius, Palaiseau Cedex, France) and was applied at a flow rate of 1 ml/min on to a 5 ml Talon-Superflow cobalt-affinity resin column (BD Clontech, St Quentin-en-Yvelines Cedex, France), pre-equilibrated with buffer B (25 mM Tris/HCl, pH 8.0/500 mM NaCl/2 mM $MgCl_2$) and connected to an ÄKTAexplorer system (Amersham Biosciences, Little Chalfont, Bucks., U.K.). The column was washed with buffer B plus 10 mM imidazole until the baseline (A_{280}) was reached. Proteins were eluted from the column with a 10–200 mM imidazole gradient in buffer B at a flow rate of 2 ml/min. Fractions were analysed by SDS/PAGE, and NBD1 (eluted between 70 and 100 mM imidazole) was collected. After concentration with a centrifugal filter (Ultrafree; Millipore, St Quentin-en-Yvelines Cedex, France) to a final volume of 10 ml, NBD1 was dialysed against buffer C [25 mM Tris/HCl, pH 8.0/10 mM NaCl/2 mM $MgCl_2$/7 mM 2ME (2-mercaptoethanol)]. The dialysed sample was filtered (0.22 μm Millex filter, Millipore) before application on to 6 ml of ResourceQ anion-exchanger resin (Amersham Biosciences), pre-equilibrated with buffer D (25 mM Tris/HCl, pH 8.0/20 mM NaCl/2 mM $MgCl_2$/7 mM 2ME). Proteins were eluted with a linear gradient of 20–400 mM NaCl in buffer D at a flow rate of 6 ml/min, and NBD1 emerged at 60–90 mM NaCl. After concentration, protein samples (15–20 mg of NBD1 in 500 μl) were loaded on to a Superdex 75HR 10/30 column (Amersham Biosciences), equilibrated with buffer E (25 mM Tris/HCl, pH 8.0/150 mM NaCl/2 mM $MgCl_2$/7 mM 2ME). Elution profile was monitored at 280 nm using a flow rate of 0.3 ml/min. After SDS/PAGE analysis, NBD1 was collected and stored at − 20 °C at an NBD1 concentration of 0.5–1 mM in buffer D containing 50 % (v/v) glycerol. For the production of thrombin-cleaved NBD1, 30 mg of His_6–NBD1, purified on Talon-Superflow cobalt was incubated with 250 units of human thrombin in buffer D plus 2.5 mM $CaCl_2$ overnight at 4 °C. After digestion, the non-fused product followed the same purification procedure on ResourceQ and Superdex columns. Protein concentrations were determined with the Bio-Rad protein assay using BSA as a standard. SDS/PAGE was performed using a 15:0.37 acrylamide/bisacrylamide gel and stained with Coomassie Blue. Molecular-mass markers were from Amersham Biosciences.

ATPase activity

ATPase activity of NBD1 was determined at 30 °C by following the amount of radiolabelled P_i released during ATP hydrolysis. The [^{33}P]P_i produced was isolated from [γ-^{33}P]ATP (Amersham Biosciences) using the charcoal method [11]. Standard reaction mixture (20 μl) contained, unless otherwise indicated, 50 mM Tris/HCl (pH 8.0), 100 mM NaCl, 5 mM $MgCl_2$, 5 % (v/v) glycerol and 40–80 μM purified NBD1. (Exceptions are mentioned in the Figure legends.) The reaction was started by adding [γ-^{33}P]ATP (1.2 mM, 15–30 Bq/pmol). The reaction was stopped at the indicated time at 4 °C by adding 400 μl of a 4 % suspension of activated charcoal in 20 mM H_3PO_4 to aliquots (3 μl) of the reaction mixture. After centrifugation, 200 μl of supernatant was mixed with 3 ml of OptiPhase HiSafe 3 (PerkinElmer LifeSciences, Great Shelford, Cambridge, U.K.) and counted in a Wallac 1414 liquid-scintillation counter. The ATP-specific activity was controlled and the amount of [^{33}P]P_i produced was determined to evaluate the rate of ATP hydrolysis.

Fluorescence measurements

Binding of the nucleotide was monitored by changes in the intrinsic tryptophan fluorescence of NBD1. Experiments were performed in a 1 ml fluorimeter cuvette at 16 °C using an FS 2500 fluorescence spectrophotometer (Hitachi, Tokyo, Japan), with spectral bandwidths of 2.5 and 5 nm for excitation and emission respectively. NBD1 protein was diluted to 1–2 μM in 1 ml of a buffer containing 25 mM Tris/HCl (pH 8.0), 100 mM NaCl and 10 mM $MgCl_2$, supplemented with increasing concentrations of ATP/ADP. All spectra were corrected for buffer fluorescence and for dilution (never exceeding 2 % of the original volume). Excitation wavelength was adjusted to 292 nm and emission was scanned over the range 300–500 nm.

NMR studies

Two-dimensional ^{15}N-^{1}H TROSY (transverse relaxation-optimized spectroscopy) NMR spectra were recorded on a Varian INOVA 600 MHz spectrometer equipped with a triple-resonance ^{1}H/^{13}C/^{15}N 5-mm gradient probe, in the presence of 10 % (v/v) $^{2}H_2O$, at 293 K, using the States-TPPI acquisition mode. Water resonance was suppressed with a WATER-GATE sequence. Data were processed on a Silicon Graphics workstation using the Vnmr software, including shifted sine-bell apodization functions in both dimensions, appropriate phase correction, zero filling and Fourier transformation. ^{1}H chemical shifts were referenced to external 2,2-dimethyl-2-silapentane-5-sulphonic acid at 0 p.p.m. ^{15}N chemical shifts were referenced indirectly using the ^{1}H/^{15}N frequency ratios of the zero point [12]. Proton and ^{15}N spectral widths were 8000 and 1920 Hz respectively. The NBD1 protein sample concentration was 500 μM in 400 mM phosphate buffer at pH 6.3. ^{15}N-^{1}H TROSY spectra consisted of 256 FIDs of 16 scans each and recorded on 2024 time-domain points. For interaction

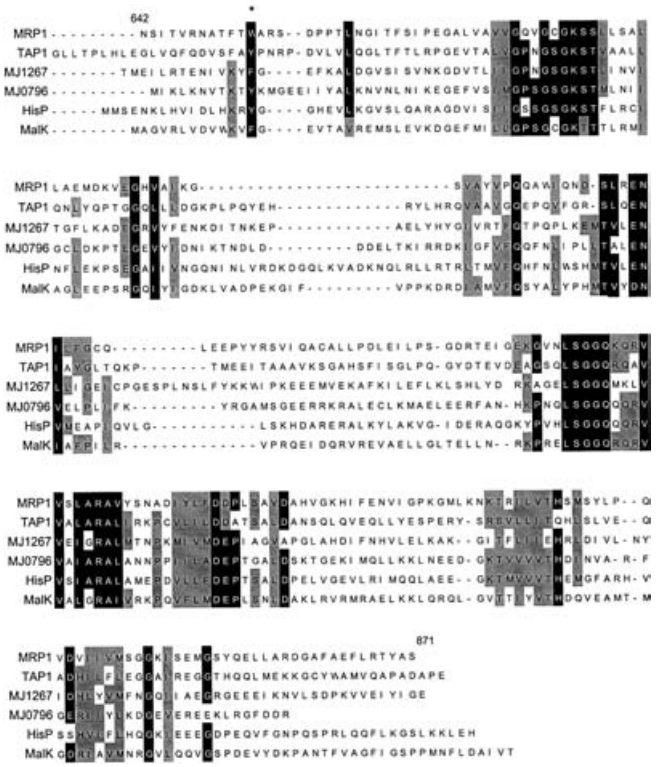

Figure 1 Sequence alignment of NBD1 of MRP1 with NBDs of known structures

Homology-based sequence alignment of NBDs of ABC transporters. Numbers refer to the sequence of MRP1. Human cTAP1 (C-terminal ABC ATPase domain of TAP1, where TAP1 stands for transporter associated with antigen processing 1) [15], *Methanococcus jannaschii* MJ1267 [16], *M. jannaschii* MJ0796 [17], *Salmonella typhimurium* HisP [13] and *Thermococcus litoralis* MalK [14]. The asterisk indicates the position of Trp^{653}.

experiments between ATP and NBD1, ATP was added at a 1 mM concentration. For experiments in the presence of magnesium, $MgCl_2$ was added at a concentration of 2 mM.

RESULTS

Design of the recombinant MRP1-NBD1 fragment

Characterization of NBD1 first requires defining its boundaries within the complete MRP1 sequence; we have used sequence alignment with NBD domains of known sequences and structures [13–17] (Figure 1). According to this alignment, we expressed the fragment Asn^{642} to Ser^{871} for NBD1 of MRP1. The retained sequence contains the complete set of secondary-structure elements that appear to be necessary for the domain to adopt a native-like three-dimensional structure. The pET28a vector was chosen to overproduce the NBD1 domain in *E. coli* as an N-terminal His_6-tagged protein. The construction adds a short sequence of 20 amino acids at the N-terminus: MGSSHHHHH-HSSGLVPRGSH that can be cleaved by thrombin treatment. The His_6-fused product (250 residues) and the non-fused NBD1 (233 residues) have theoretical molecular masses of 27 and 25.2 kDa respectively.

Production and purification of the MRP1-NBD1 domain in a monomeric state

The NBD1 domain was highly overexpressed after induction with IPTG when cells were grown in a rich medium (2YT). Lowering the induction temperature from 37 to 16 °C and extending the induction period from 4–5 h to overnight increased the amount of soluble NBD1. For the ^{15}N-labelled protein, cells were grown at 28 °C in minimal medium. After induction by IPTG, NBD1 was expressed as the major protein product in the total cell extract (Figure 2A, lane 3) when compared with non-induced bacterial cultures (Figure 2A, lane 2).

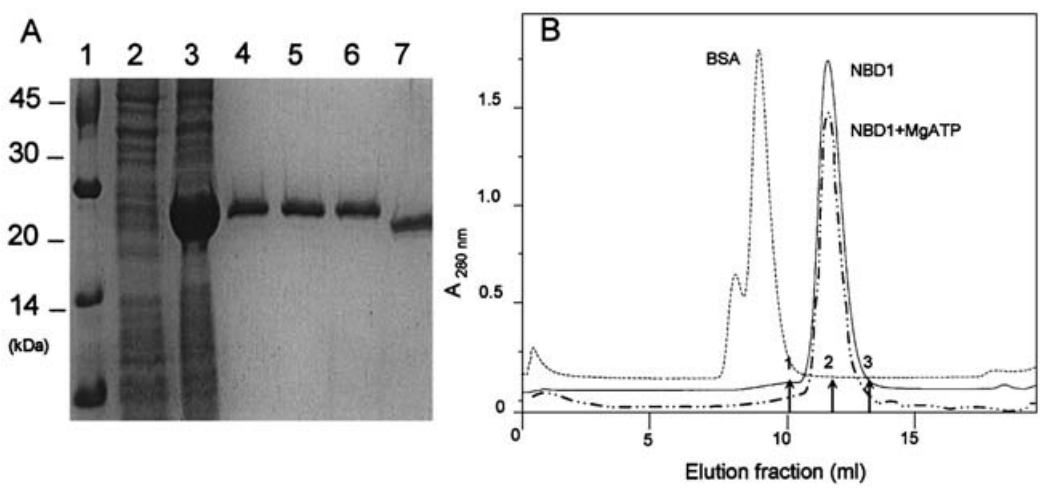

Figure 2 Expression and purification of NBD1-MRP1

(**A**) NBD1 protein was purified as described in the Materials and methods section and each purification step was analysed by SDS/PAGE (15 % gel) and Coomassie Blue staining. Lane 1, protein molecular-mass standards; Lane 2, total bacterial proteins before induction; lane 3, total bacterial proteins of IPTG-induced cells; lane 4, 1 μg of His_6–NBD1 purified on cobalt-chelating resin; lane 5, 1 μg of His_6–NBD1 after the ResourceQ purification step; lane 6, 1 μg of His_6–NBD1 after the Superdex 75 purification step; lane 7, 1 μg of non-fused NBD1 obtained by thrombin treatment. (**B**) Chromatographic profiles of Superdex 75 column showing the elution of 27 kDa NBD1-MRP1 in the absence (—) and presence (·–·–·–·) of 0.3 mM ATP in the buffer. A separate chromatographic profile of 67 kDa BSA (- - -) indicates that the Superdex 75 column would efficiently resolve the NBD1 monomer from eventual dimers. The Superdex 75 column was calibrated with other proteins (indicated by arrows): 1, 43 kDa ovalbumin; 2, 25 kDa chymotrypsinogen A; 3, 13.7 kDa RNase A. Protein concentration was recorded at A_{280}.

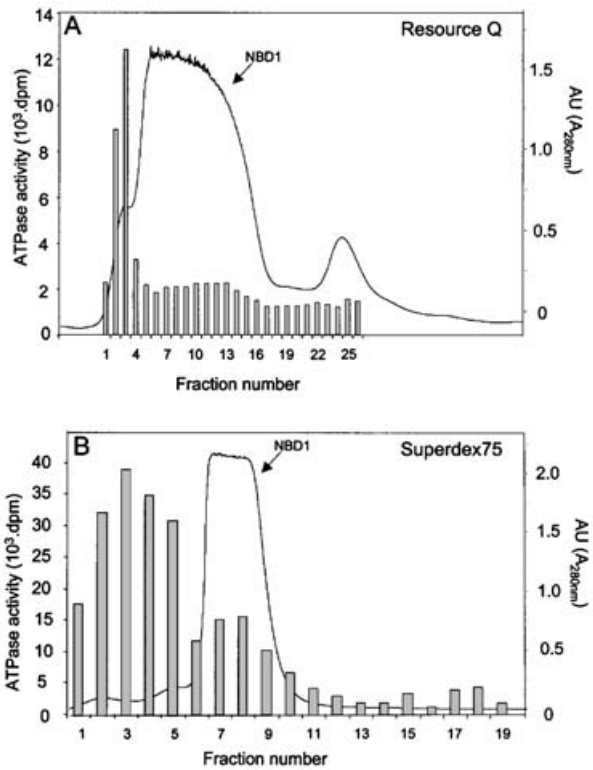

Figure 3 ATPase activity measured on NBD1 chromatographic profiles

NBD1 samples purified on cobalt-affinity resin were applied on to ResourceQ 6 ml anionic-exchanger (**A**) and gel-filtration Superdex 75HR 10/30 (**B**) columns. Protein elution was followed by A_{280} (line curve). High amounts of NBD1 were loaded on to both columns to allow detection of ATPase activity with a good sensitivity. In these experiments, protein concentration was measured in each fraction with the Bio-Rad protein assay. ATPase activity was followed on 25 μl of aliquots of each fraction by adding 5 μl of [γ-^{33}P]ATP (final concentration 0.3 mM, 22 Bq/pmol) to start the reaction. ATPase activity (shaded bars) was monitored by measuring the amount of [^{33}P]P_i produced during 4 h at 30 °C as described in the Materials and methods section. AU, absorbance unit.

All the buffers employed during the protein extraction, purification and storage procedures were devoid of any detergent or denaturant. The first purification step of NBD1 was performed using a cobalt-chelating resin (Figure 2A, lane 4). Although no contaminants are visible on the Coomassie-Blue-stained gel after the first purification step, a second purification step on an anionic column (Figure 2A, lane 5) proved to be essential to eliminate contaminating nucleotidases for ATPase activity studies on NBD1 (see below and Figure 3).

To analyse the apparent molecular mass of NBD1, Superdex 75 (fractionation sizes, 3–70 kDa) and Superdex 200 (fractionation sizes, 10–600 kDa) columns were used. The protein (Figure 2A, lane 6) eluted at an apparent molecular mass corresponding to a monomeric NBD1 domain (Figure 2B). Less than 3 % of the total amount of protein was detected at higher molecular masses. The presence of MgATP in the protein sample or in chromatographic buffers does not modify this monomeric state (Figure 2B). Native-gel electrophoresis also confirmed that a single band was observed and no oligomerization of NBD1 could be detected.

The purification yields were 40 mg/l NBD1 from a culture in 2YT medium and 15 mg/l in minimal medium. The His_6 tag of NBD1 can be cleaved without loss of material and the non-fused NBD1 run at the expected size on the SDS/polyacrylamide gel (Figure 2A, lane 7). No significant differences in the enzymic

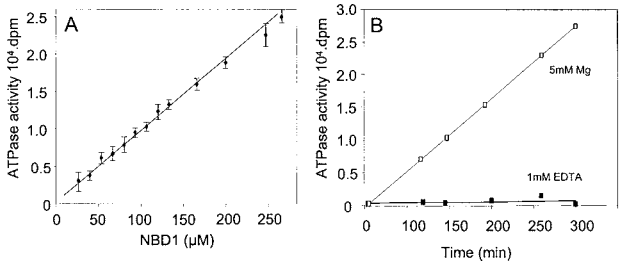

Figure 4 NBD1 ATPase activity and influence of magnesium

The intrinsic ATPase activity was determined with three-step purified NBD1 preparations using [γ-^{33}P]ATP as substrate. (**A**) ATPase activity of NBD1 was studied as a function of its concentration in standard buffer after 240 min of incubation at 30 °C. (**B**) The ATPase activity of NBD1 (80 μM) was determined in 40 μl of buffer (50 mM Tris/HCl, pH 8/100 mM NaCl/5 % glycerol) in the presence of 5 mM $MgCl_2$ (□) or in the absence of magnesium, but with 1 mM EDTA (■). Aliquots (5 μl) were withdrawn at indicated times of the kinetics.

parameters were observed between His_6-fused and -cleaved NBD1.

ATPase activity of the purified MRP1-NBD1 domain

To determine the *in vitro* ATPase activity of the isolated NBD1, we quantified the [^{33}P]P_i produced during the hydrolysis of [γ-^{33}P]ATP by NBD1. We monitored the ATPase activity for each fraction at every purification step and found that it was necessary to perform three chromatographic steps to avoid contamination with *E. coli* nucleotidases. We checked that the loss of the ATPase activity was not due to a partial inactivation of NBD1 (Figure 3): high ATPase activities were detected, and their maximum did not overlap with fractions containing the NBD1 domain. The rate of ATP hydrolysis by NBD1 was found to be very low, of the order of 10^{-5} s^{-1} [0.02 nmol of $P_i \cdot$ (mg of NBD1)$^{-1} \cdot$ min^{-1}]. Therefore incubation times were prolonged for several hours, and we controlled the stability of the enzyme over this period of time. As shown in Figure 4(A), the hydrolysis kinetics vary linearly with the NBD1 concentration. We observed a 25 % decrease in activity when NaCl concentration increased from 10 to 250 mM. The activity was only slightly affected over the pH range 7–9. Consistent with previous reports, ATPase activity was fully dependent on the presence of Mg^{2+} (Figure 4B), since no activity could be detected in the presence of EDTA. No significant difference in activity was observed between the His_6–NBD1 and the non-fused NBD1 preparations, demonstrating that the His tag was not perturbing our assay.

To evaluate the enzymic parameters of the NBD1-induced ATP hydrolysis (Figure 5), the activity was measured as a function of ATP concentration, and Michaelis–Menten curves were determined. The values of V_{max} and K_m were 5×10^{-5} s^{-1} and 833 μM respectively. The ATPase activity of this MRP1-NBD1 domain appears to be very low compared with previously published results, characterizing isolated NBD domains of ABC proteins. The V_{max} value obtained shows that a single turnover (1 ATP molecule hydrolysed per NBD1) would take several hours under optimal conditions and more than 1 day at the experimental rate of 10^{-5} s^{-1}.

NMR analysis

All NMR spectra displayed peaks with relatively large linewidths, but compatible with the mass of this protein (27 kDa). The two-dimensional ^{15}N-^{1}H TROSY spectrum of NBD1 shown in Figure 6(A) correlates all amide protons to its attached nitrogen

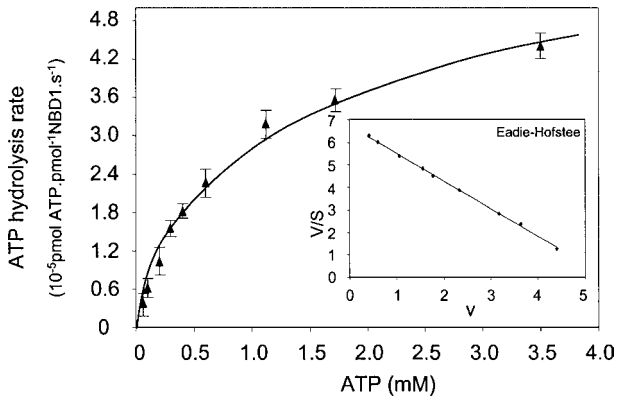

Figure 5 Enzymic parameters of NBD1 ATP hydrolysis

The rate of ATP hydrolysis was measured as a function of ATP concentration for an 80 μM NBD1 sample, as described in the Materials and methods section. Each point corresponds to the hydrolysis rate determined kinetically for 180 min. Inset shows the Eadie–Hofstee plot.

[18]. This spectrum presents a wide spectral dispersion in both dimensions. The absence of a central cluster of unresolved resonances, in the NMR spectra, as observed in unfolded proteins or in molten globules, clearly demonstrates that the protein is folded. This ^{15}N-^{1}H TROSY spectrum remained unaffected by the addition of two equivalents of Mg^{2+} (results not shown). Two peaks were observed in the chemical shifts range, where tryptophan N-Hε side-chain correlations are usually observed, as shown in rectangles in Figures 6(A) and 6(B). The position of N-Hε in the tryptophan side chain is given in Figure 6(D). Two tryptophan residues are present in the primary sequence of NBD1, at positions 653 and 717. In the presence of ATP, one of the two peaks disappears as a consequence of line broadening (Figure 6C). This modification indicates that one of the two tryptophan residues is involved in ATP binding. However, the overall line width observed in the spectrum was not affected by the presence of ATP, and remained compatible with a molecular mass of 27 kDa. Presence of significant amounts of dimers or larger oligomers would lead to much larger line widths with hardly any signal detectable.

The sequence alignment of Figure 1 allowed assignment of these two tryptophan residues, Trp^{653} and Trp^{717}. Trp^{653} in MRP1 is aligned with an aromatic residue (Tyr or Phe). In the known crystal structures of NBD–ATP (or NBD–ADP) complexes, these residues are involved in hydrophobic stacking with the adenine ring. On the contrary, Trp^{717} belongs to a more variable region situated far from the ATP molecule. We concluded that the aromatic ring of Trp^{653} of NBD1 is in interaction with ATP.

In addition, a few other resonances of the Trosy spectrum are affected in frequency or intensity by the presence of Mg^{2+} and ATP. In particular, two resonances situated in the region of N-H correlations of glycine residues (at low ^{15}N chemical shift) are shifted in the presence of ATP, and then disappear when magnesium is added. These resonances are shown in Figure 6(A). They could correspond to the glycine residues of the Walker A consensus sequence, described previously to interact with the phosphate group of ATP in ABC transporters [13].

Fluorescence measurement of the nucleotide binding to the MRP1-NBD1 domain

Identification of Trp^{653} as a residue involved in ATP binding suggested that it is possible to determine the NBD1–ATP dissociation

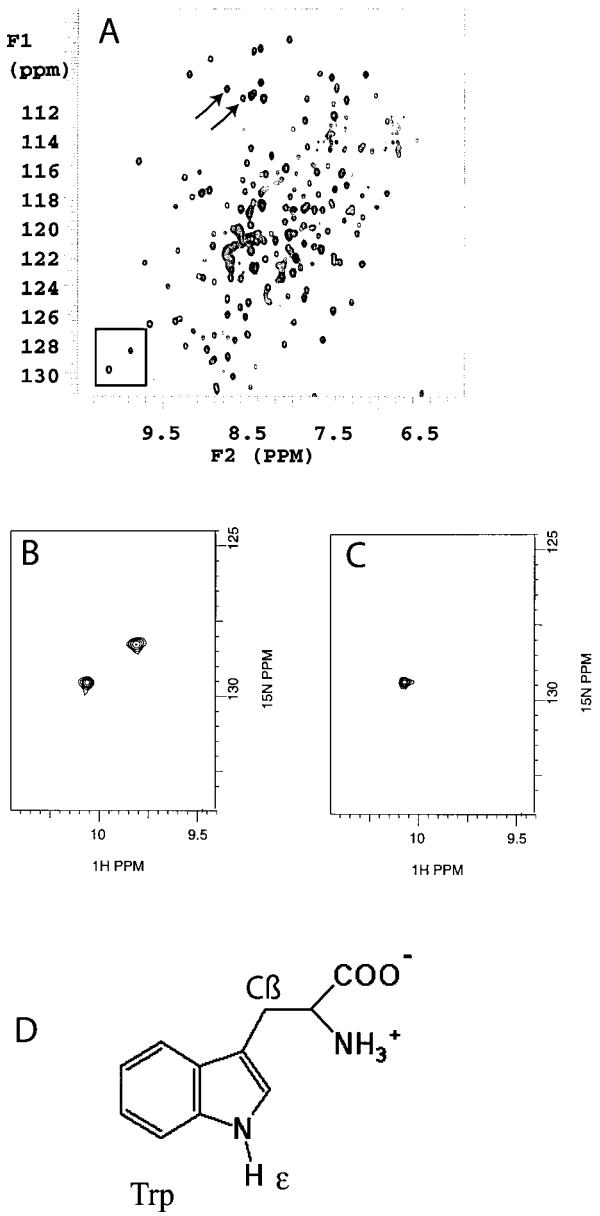

Figure 6 Heteronuclear spectra of NBD1

(**A**) ^{15}N-^{1}H Trosy-HSQC spectrum of NBD1. The black rectangle corresponds to the zoom shown in (**B**, **C**). The two arrows indicate resonances that shifted in the presence of ATP, and disappeared when magnesium was added. (**B**) Zoom of the black rectangle in (**A**). (**C**) Same zoom in the presence of ATP and magnesium ion. (**D**) Structure of a tryptophan side chain, showing the position of the Hε proton.

constant by measuring the intrinsic tryptophan fluorescence of NBD1. Figure 7(A) shows that titration by ATP in the presence of magnesium ions decreased the fluorescence intensity by 50% before reaching saturation. The decrease in intrinsic fluorescence at 344 nm was monitored under the same conditions for ATP or ADP and allowed the determination of $K_{d(ATP)}$ value of 118 ± 18 μM (Figure 7B) and a similar affinity for ADP ($K_{d(ADP)} = 139 \pm 15$ μM; results not shown). Interestingly, the binding of the nucleotide to NBD1 was affected by the absence of $MgCl_2$ from the buffer. As illustrated in Figure 7(C), using an almost-saturating ATP concentration of 1 mM, the decrease in tryptophan fluorescence is much lower in the presence

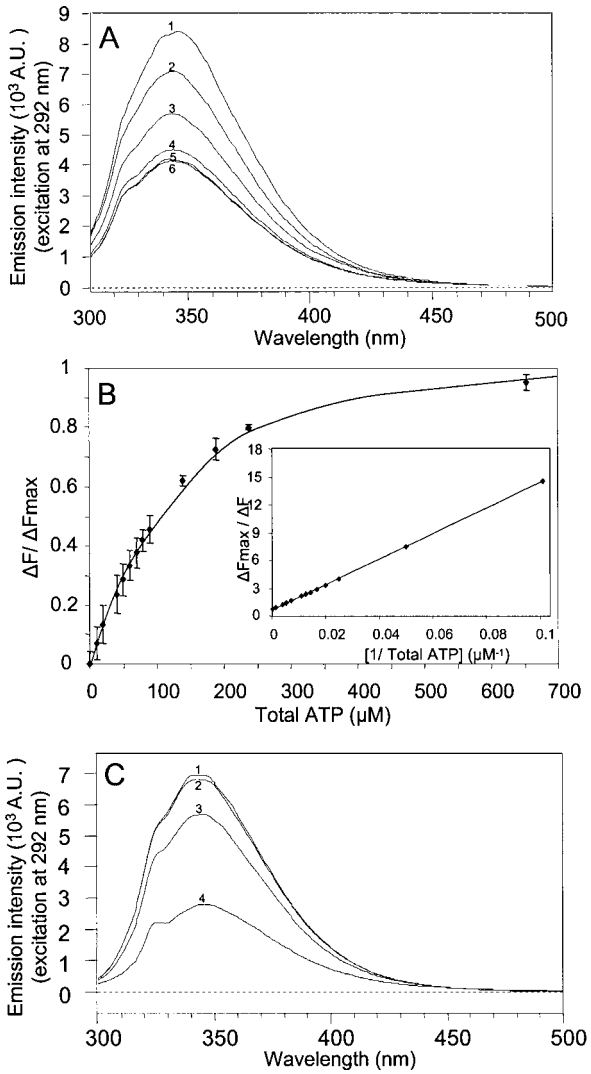

Figure 7 Characterization of NBD1–ATP interaction by tryptophan intrinsic fluorescence

(**A**) Fluorescence spectra of 1 μM nucleotide-free NBD1 (spectrum 1) and in the presence of increasing concentrations of ATP (60 μM, spectrum 2; 170 μM, spectrum 3; 500 μM, spectrum 4; 1.4 mM, spectrum 5; 3 mM, spectrum 6) as described in the Materials and methods section. A.U., arbitrary unit. (**B**) Maximum quenching at 344 nm obtained after saturation of NBD1 by ATP ($\lambda_{ex} = 292$ nm). Values are expressed as a percentage of the maximal peak fluorescence quenching, $\Delta F/\Delta F_{max}$. The binding constant K_d for the NBD–ATP complex was determined from the double-reciprocal plot as shown in the inset. (**C**) Influence of magnesium on ATP binding to NBD1 in a buffer containing 25 mM Tris/HCl (pH 8.0), 100 mM NaCl and one of the following: 1 mM EDTA (spectrum 1), 100 μM ATP + 1 mM EDTA (spectrum 2), 1 mM ATP + 1 mM EDTA (spectrum 3) and 1 mM ATP + 1 mM EDTA + 5 mM $MgCl_2$ (spectrum 4).

of EDTA when compared with the value obtained in the presence of an excess of $MgCl_2$. These results indicate that magnesium increases the efficiency of the nucleotide–NBD1 complex formation.

DISCUSSION

MRP1-NBD1 is purified as a soluble and monomeric protein

Results of the present study show that MRP1-NBD1 can be expressed very efficiently in *E. coli*, and that a highly purified protein can be prepared as a folded and exclusively monomeric protein. Moreover, characterization of NBD1 reveals that the His_6 tag fused at the N-terminal can be removed by thrombin treatment without loss of solubility or stability. A limited number of studies have reported the expression and purification of the isolated NBD1 of MRP1. Gao et al. [6] produced the MRP1-NBD1 domain (Arg^{617} to Ala^{932}) in insect cells as a non-fused soluble protein, but no further purification steps were described for this protein fragment. Kern et al. [8] studied an NBD1 domain encompassing Arg^{647} to Ile^{846}, expressed in *E. coli* as a fusion protein with MBP (maltose-binding protein) at the N-terminus, and a His_6 tag at the C-terminus. The resulting fused protein (66 kDa) was shown to form oligomers with apparent molecular masses of more than 2000 kDa. Compared with our protein, this construct lacks approx. 25 residues at the C-terminus. These residues are involved in secondary-structure elements in NBDs of known structures (referred to as α8 and α9 in the structure of HisP (histidine permease) [13]). In contrast with the Asn^{642} to Ser^{871} MRP1 fragment, the absence of these elements might expose hydrophobic regions of the protein, leading to aggregation. Recent works have described production of the fused NBD1 with different N- and C-terminal ends: NBD1 fragments encompassing either Asp^{657} to Asn^{819} fused to MBP and the FLAG epitope [10] or residues Lys^{614} to Lys^{959} fused to MBP or glutathione S-transferase [9]. Unfortunately, no specific description of the monomeric or oligomeric state of these one-step purified protein preparations was available in these reports. Hence, we cannot evaluate the role of the 52 residues deleted or the 88 residues added at the C-terminal end as compared with our NBD1 fragment. Although the type of expression system might influence the tendency to form oligomers and aggregates, our results demonstrate that a careful design of the domain also plays a crucial role.

Trp^{653} is involved in the NBD1–ATP complex formation

The close interaction between Trp^{653} and the adenine ring of ATP identified by NMR in the present study recalls the stacking of the adenine ring of ADP/ATP with an aromatic residue in the known NBD crystal structures of ABC transporters [13,15–17]. This indicates that the local binding site of NBD1 of MRP1 is probably very similar to those described previously. The mutation of the equivalent residue in HisP (Tyr^{16}) abolishes both ATP binding and histidine transport [19]. Unexpectedly, certain mutations of aromatic residues, which are equivalent in NBD1 and NBD2 of CFTR (cystic fibrosis transmembrane conductance regulator) to Tyr^{16} in HisP (and to Trp^{653} in MRP1), had no influence on the CFTR channel function [20]. This suggests that the ATP-binding mode could be different in CFTR from that observed in MRP1, which is somewhat surprising in the same subfamily of ATP transporters (the NBDs of CFTR and MRP1 share 40% sequence identity). This conserved aromatic residue is not found in the structures of proteins presenting less sequence identity such as BtuCD or Rad50 [21,22].

The NBD1–nucleotide complex formation was studied by intrinsic fluorescence of the protein. To our knowledge, this is the first direct measurement of the MRP1-NBD1–nucleotide affinity, avoiding the use of fluorescent nucleotide analogues. Titration curves of NBD1 by MgATP or MgADP gave quite similar K_d values for both nucleotides (118 μM for ATP and 139 μM for ADP). A somewhat higher affinity was described by competitive displacement of TNP-ATP [2′(3′)-*O*-2,4,6-trinitrophenyl-ATP] on MBP-fused NBD1 [8] and a lower affinity for ADP when compared with ATP was proposed, using a shorter NBD1 construct, as the result of ATPase competition experiments [10]. However, as shown in sequence alignment (Figure 1), our NBD1

includes the first β-sheet described in known three-dimensional structures. This structural element contains Trp^{653}.

Isolated NBD1 has a very low ATPase activity

The intrinsic ATPase activity of the NBD1 domain was found to be extremely low, up to 660 times lower when compared with previously published results on recombinant MRP1-NBD1. This low catalytic activity, evaluated over the range of 10^{-5} s^{-1}, appears to be an intrinsic property of NBD1 protein. We found a V_{max} value for the ATPase activity of 0.1 nmol of $P_i \cdot mg^{-1} \cdot min^{-1}$ as compared with the reported V_{max} values of 6–10 and 66 nmol of $P_i \cdot mg^{-1} \cdot min^{-1}$ for fused NBD1 [8–10]. These 2–3 orders of magnitude differences in the NBD1 ATPase activity of MRP1 could be a consequence of differences in (i) sizes of the generated domain, (ii) fusion partner and (iii) monomeric or oligomeric state of the protein. However, a very important factor seems to be the degree of purity of NBD1 preparations. We evaluated the ATPase activity of NBD1 during its purification (Figure 3): it was necessary to perform three chromatographic steps to avoid contaminations with *E. coli* nucleotidases. The ATPase activities, obtained after the first purification step, were not always constant, and were often higher than the activity observed after the second or third purification step. This indicates that, after the first chromatography step, contaminant ATPases that were not detectable on the Coomassie-Blue-stained gels contribute to the overall ATPase activity. Consequently, our results show that the ATPase activity of highly purified NBD1 is very low and its maximum rate shows that it would take several hours for a single turnover to be reached.

The NBD1 ATPase activity is also several orders of magnitude lower than that reported for the full-length protein. ATPase values from 10 to 460 nmol of $P_i \cdot mg^{-1} \cdot min^{-1}$ were measured for purified human MRP1 [23,24]. Our results would indicate that NBD1 has a low contribution to the overall ATPase activity of MRP1. However, it is not clear whether the ATPase activity of NBD1 in full-length MRP1 is also low or not, or whether this low activity of the recombinant NBD1 is a consequence of lack of interactions with other parts of the molecule, such as the LSVGQ signature sequence of NBD2. For P-glycoprotein, the two NBDs are highly similar in sequence, ATP hydrolysis occurring alternatively at each NBD [25]. On the contrary, in MRP1, the two NBDs are significantly more divergent, and were not found to be functionally equivalent [6,7,26–28]. It has been suggested that NBD1 would be the site for ATP binding, leading to a positive allosteric stimulation of ATP hydrolysis at NBD2 [29,30]. The very low intrinsic ATPase activity of NBD1 observed in the present study is consistent with that model.

Role of magnesium in the nucleotide binding/hydrolysis cycle

Modifications described above in the NMR spectra and involving Trp^{653} did not require the presence of magnesium. The magnesium ion is expected to interact with the γ-phosphate of ATP and the aspartic residue of the Walker B sequence, to catalyse hydrolysis. However, this ion should not be critical for the binding of the adenine and ribose groups. On the contrary, the modifications observed in the region of glycine residues and proposed to be glycine residues of Walker A are dependent on magnesium. The glycine residues of Walker A (e.g. Gly^{42} and Gly^{44} of HisP, corresponding to Gly^{681} and Gly^{683} of MRP1) have been described to interact with the phosphate groups of ATP. The NMR results are consistent with induction of local structural rearrangement in the presence of magnesium, allowing correct phosphate binding. Similarly, the decrease in tryptophan fluorescence observed by the NBD1–ATP complex formation was greatly influenced by the presence of magnesium. Our experiments indicate that the presence of magnesium was not essential for the binding of the nucleotide, but increases the affinity of the NBD1 for ATP and plays a crucial role in the mechanism of the ATP hydrolysis reaction.

Gel-filtration experiments, native electrophoresis and NMR results all showed that the presence of magnesium and ADP and/or ATP did not modify the monomeric state of NBD1. Also, the rate of ATP hydrolysis displayed a linear response with protein concentration, showing that the intrinsic ATPase activity of NBD1 did not depend on dimer formation. The inability of NBD1 to self-associate probably prevents the formation of intermolecular NBD1–NBD1 dimers in full-length MRP1 molecules, thus favouring an intramolecular NBD1–NBD2 interaction believed to be necessary for the correct activation of ABC transporters. This characteristic was not observed for ABC transporters presenting a single NBD, such as HisP [31] or BtuD [22].

The lower affinity of the isolated NBD1 for ATP observed in the present study when compared with that of the full-length MRP1 (the K_d value is 8-fold higher for NBD1 than for MRP1) [29] could be due to the presence of additional interactions at the NBD1–NBD2 heterodimer interface in MRP1. In particular, the ABC signature of NBD2 could stabilize the nucleotide binding at NBD1. Studies of the ability of recombinant NBD1 and NBD2 to interact with each other and to influence their ATP binding/hydrolysis cycle are necessary to understand the activation mechanism of the full-length transporter and to describe the interface of this heterodimer.

We thank the association 'Vaincre la mucoviscidose' for financial support and a post-doctoral grant to F. D., the association ABCF-Protein for a grant to M. O. and the Région Ile-de-France for financial support for the Varian 600 MHz spectrometer of Institut Pasteur. We thank Dr P. Genne (Oncodesign) for the gift of HL60/ADR cells, Emeric Miclet and Jérome Bignon for scientific discussions and Muriel Lainé for a critical reading of the manuscript.

REFERENCES

1 Holland, I. B., Cole, S. P., Kuchler, K. and Higgins, C. F. (eds.) (2003) ABC Proteins from Bacteria to Man, Academic Press, London
2 Hipfner, D. R., Deeley, R. G. and Cole, S. P. (1999) Structural, mechanistic and clinical aspects of MRP1. Biochim. Biophys. Acta **1461**, 359–376
3 Dean, M., Rzhetsky, A. and Allikmets, R. (2001) The human ATP-binding cassette (ABC) transporter superfamily. Genome Res. **11**, 1156–1166
4 Borst, P., Evers, R., Kool, M. and Wijnholds, J. (2000) A family of drug transporters: the multidrug resistance-associated proteins. J. Natl. Cancer Inst. **92**, 1295–1302
5 Hipfner, D. R., Almquist, K. C., Leslie, E. M., Gerlach, J. H., Grant, C. E., Deeley, R. G. and Cole, S. P. (1997) Membrane topology of the multidrug resistance protein (MRP). A study of glycosylation-site mutants reveals an extracytosolic NH_2 terminus. J. Biol. Chem. **272**, 23623–23630
6 Gao, M., Cui, H. R., Loe, D. W., Grant, C. E., Almquist, K. C., Cole, S. P. and Deeley, R. G. (2000) Comparison of the functional characteristics of the nucleotide binding domains of multidrug resistance protein 1. J. Biol. Chem. **275**, 13098–13108
7 Hou, Y. X., Cui, L., Riordan, J. R. and Chang, X. B. (2002) ATP binding to the first nucleotide-binding domain of multidrug resistance protein MRP1 increases binding and hydrolysis of ATP and trapping of ADP at the second domain. J. Biol. Chem. **277**, 5110–5119
8 Kern, A., Felfoldi, F., Sarkadi, B. and Varadi, A. (2000) Expression and characterization of the N- and C-terminal ATP-binding domains of MRP1. Biochem. Biophys. Res. Commun. **273**, 913–919
9 Cool, R. H., Veenstra, M. K., van Klompenburg, W., Heyne, R. I., Muller, M., de Vries, E. G., van Veen, H. W. and Konings, W. N. (2002) S-decyl-glutathione nonspecifically stimulates the ATPase activity of the nucleotide-binding domains of the human multidrug resistance-associated protein, MRP1 (ABCC1). Eur. J. Biochem. **269**, 3470–3478
10 Wilkes, D. M., Wang, C., Aristimuno, P. C., Castro, A. F. and Altenberg, G. A. (2002) Nucleotide triphosphatase activity of the N-terminal nucleotide-binding domains of the multidrug resistance proteins P-glycoprotein and MRP1. Biochem. Biophys. Res. Commun. **296**, 388–394

11 Parrini, M. C., Jacquet, E., Bernardi, A., Jacquet, M. and Parmeggiani, A. (1995) Properties and regulation of the catalytic domain of Ira2p, a *Saccharomyces cerevisiae* GTPase-activating protein of Ras2p. Biochemistry **34**, 13776–13783
12 Wishart, D. S., Bigam, C. G., Yao, J., Abildgaard, F., Dyson, H. J., Oldfield, E., Markley, J. L. and Sykes, B. D. (1995) ^{1}H, ^{13}C and ^{15}N chemical shift referencing in biomolecular NMR. J. Biomol. NMR **6**, 135–140
13 Hung, L. W., Wang, I. X., Nikaido, K., Liu, P. Q., Ames, G. F. and Kim, S. H. (1998) Crystal structure of the ATP-binding subunit of an ABC transporter. Nature (London) **396**, 703–707
14 Diederichs, K., Diez, J., Greller, G., Muller, C., Breed, J., Schnell, C., Vonrhein, C., Boos, W. and Welte, W. (2000) Crystal structure of MalK, the ATPase subunit of the trehalose/maltose ABC transporter of the archaeon *Thermococcus litoralis*. EMBO J. **19**, 5951–5961
15 Gaudet, R. and Wiley, D. C. (2001) Structure of the ABC ATPase domain of human TAP1, the transporter associated with antigen processing. EMBO J. **20**, 4964–4972
16 Karpowich, N., Martsinkevich, O., Millen, L., Yuan, Y., Dai, P. L., MacVey, K., Thomas, P. J. and Hunt, J. F. (2001) Crystal structures of the MJ1267 ATP binding cassette reveal an induced-fit effect at the ATPase active site of an ABC transporter. Structure **9**, 571–586
17 Yuan, Y. R., Blecker, S., Martsinkevich, O., Millen, L., Thomas, P. J. and Hunt, J. F. (2001) The crystal structure of the MJ0796 ATP-binding cassette. Implications for the structural consequences of ATP hydrolysis in the active site of an ABC transporter. J. Biol. Chem. **276**, 32313–32321
18 Pervushin, K., Riek, R., Wider, G. and Wuthrich, K. (1997) Attenuated T2 relaxation by mutual cancellation of dipole–dipole coupling and chemical shift anisotropy indicates an avenue to NMR structures of very large biological macromolecules in solution. Proc. Natl. Acad. Sci. U.S.A. **94**, 12366–12371
19 Shyamala, V., Baichwal, V., Beall, E. and Ames, G. F. (1991) Structure–function analysis of the histidine permease and comparison with cystic fibrosis mutations. J. Biol. Chem. **266**, 18714–18719
20 Berger, A. L. and Welsh, M. J. (2000) Differences between cystic fibrosis transmembrane conductance regulator and HisP in the interaction with the adenine ring of ATP. J. Biol. Chem. **275**, 29407–29412
21 Hopfner, K. P., Karcher, A., Shin, D. S., Craig, L., Arthur, L. M., Carney, J. P. and Tainer, J. A. (2000) Structural biology of Rad50 ATPase: ATP-driven conformational control in DNA double-strand break repair and the ABC-ATPase superfamily. Cell (Cambridge, Mass.) **101**, 789–800
22 Locher, K. P., Lee, A. T. and Rees, D. C. (2002) The *E. coli* BtuCD structure: a framework for ABC transporter architecture and mechanism. Science **296**, 1091–1098
23 Chang, X. B., Hou, Y. X. and Riordan, J. R. (1997) ATPase activity of purified multidrug resistance-associated protein. J. Biol. Chem. **272**, 30962–30968
24 Mao, Q., Leslie, E. M., Deeley, R. G. and Cole, S. P. (1999) ATPase activity of purified and reconstituted multidrug resistance protein MRP1 from drug-selected H69AR cells. Biochim. Biophys. Acta **1461**, 69–82
25 Senior, A. E., Al-Shawi, M. K. and Urbatsch, I. L. (1998) ATPase activity of Chinese hamster P-glycoprotein. Methods Enzymol. **292**, 514–523
26 Nagata, K., Nishitani, M., Matsuo, M., Kioka, N., Amachi, T. and Ueda, K. (2000) Nonequivalent nucleotide trapping in the two nucleotide binding folds of the human multidrug resistance protein MRP1. J. Biol. Chem. **275**, 17626–17630
27 Hou, Y., Cui, L., Riordan, J. R. and Chang, X. (2000) Allosteric interactions between the two non-equivalent nucleotide binding domains of multidrug resistance protein MRP1. J. Biol. Chem. **275**, 20280–20287
28 Hou, Y. X., Riordan, J. R. and Chang, X. B. (2003) ATP binding, not hydrolysis, at the first nucleotide-binding domain of multidrug resistance-associated protein MRP1 enhances ADP.Vi trapping at the second domain. J. Biol. Chem. **278**, 3599–3605
29 Yang, R., Cui, L., Hou, Y. X., Riordan, J. R. and Chang, X. B. (2003) ATP binding to the first nucleotide binding domain of MRP1 plays a regulatory role at low nucleotide concentration whereas ATP hydrolysis at the second plays a dominant role in ATP-dependent LTC4 transport. J. Biol. Chem. **278**, 30764–30771
30 Payen, L. F., Gao, M., Westlake, C. J., Cole, S. P. C. and Deeley, R. G. (2003) Role of carboxylate residues adjacent to the conserved core Walker B motifs in the catalytic cycle of multidrug resistance protein 1 (ABCC1). J. Biol. Chem. **278**, 38537–38547
31 Nikaido, K., Liu, P. Q. and Ames, G. F. (1997) Purification and characterization of HisP, the ATP-binding subunit of a traffic ATPase (ABC transporter), the histidine permease of *Salmonella typhimurium*. Solubility, dimerization, and ATPase activity. J. Biol. Chem. **272**, 27745–27752

Received 3 July 2003/2 September 2003; accepted 3 September 2003
Published as BJ Immediate Publication 3 September 2003, DOI 10.1042/BJ20030998